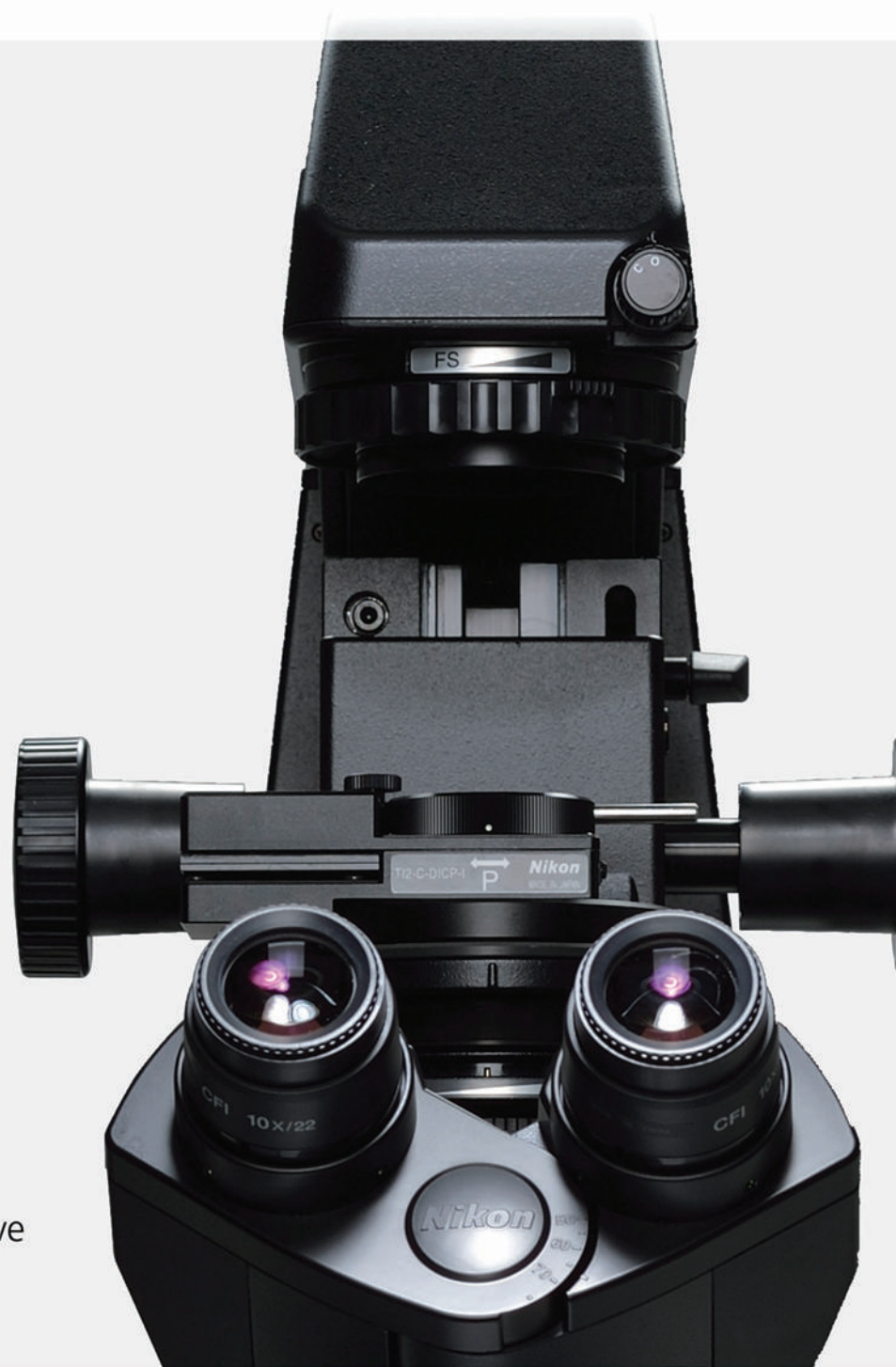




# Nikon Bioimaging Lab

Let us do the imaging for you.



The Nikon Bioimaging Lab is a state-of-the-art facility located in Cambridge, Massachusetts, that provides advanced technologies to support the burgeoning regenerative medicine and biotech sector.

For more information, visit [www.microscope.healthcare.nikon.com/bioimaging-lab](http://www.microscope.healthcare.nikon.com/bioimaging-lab)



Nikon Instruments Inc. ■ [www.microscope.healthcare.nikon.com](http://www.microscope.healthcare.nikon.com) ■ [nikoninstruments@nikon.net](mailto:nikoninstruments@nikon.net)

<sup>a</sup>Department of Neurosurgery, Qilu Hospital of Shandong University, Jinan, People's Republic of China; <sup>b</sup>Brain Science Research Institute, Shandong University, Jinan, People's Republic of China; <sup>c</sup>Key Laboratory of the Ministry of Education for Experimental Teratology, Department of Histology and Embryology, Shandong University School of Basic Medical Sciences, Jinan, People's Republic of China; <sup>d</sup>The Key Laboratory of Cardiovascular Remodeling and Function Research, Chinese Ministry of Education and Chinese Ministry of Health, the State and Shandong Province Joint Key Laboratory of Translational Cardiovascular Medicine, Qilu Hospital of Shandong University, Jinan, People's Republic of China; <sup>e</sup>Department of Neurosurgery, Yinan County People's Hospital, Linyi, People's Republic of China; <sup>f</sup>Department of Neurosurgery, PLA No. 970 Hospital, Yantai, Shandong, People's Republic of China; <sup>g</sup>Shandong University School of Medicine, Jinan, People's Republic of China; <sup>h</sup>Department of Infection Management, The Second People's Hospital of Yunnan Province, Kunming, People's Republic of China; <sup>i</sup>Department of Otorhinolaryngology, Qilu Hospital of Shandong University, Jinan, People's Republic of China; <sup>j</sup>Department of Neurosurgery, Xuanwu Hospital of Capital Medical University, Beijing, People's Republic of China; <sup>k</sup>Department of Neurosurgery, Affiliated Hospital of Jining Medical University, Jining, People's Republic of China; <sup>l</sup>KG Jebsen Brain Tumor Research Center, Department of Biomedicine, University of Bergen, Bergen, Norway

\*Contributed equally.

Correspondence: Shilei Ni, Doctor of Medicine, Qilu Hospital of Shandong University, 107#, Wenhua Xi Road, Jinan, Shandong 250012, People's Republic of China. Telephone: +8613869196590; e-mail: nishilei@sdu.edu.cn

Received May 29, 2018; accepted for publication December 11, 2018; first published online in *STEM CELLS EXPRESS* January 14, 2019.

<http://dx.doi.org/10.1002/stem.2968>

## Melatonin Enhances Proliferation and Modulates Differentiation of Neural Stem Cells Via Autophagy in Hyperglycemia

HAOYUAN LI,<sup>a,\*</sup> YANMIN ZHANG,<sup>b,c,\*</sup> SHANGMING LIU,<sup>c,d</sup> FENGPENG LI,<sup>e</sup> BENLIN WANG,<sup>f</sup> JIANJIE WANG,<sup>g</sup> LANFANG CAO,<sup>h</sup> TONGLIANG XIA,<sup>i</sup> QINGYU YAO,<sup>j</sup> HAIJUN CHEN,<sup>a</sup> YULIN ZHANG,<sup>a</sup> XIAODONG ZHU,<sup>k</sup> YANG LI,<sup>g</sup> GANG LI,<sup>a,b</sup> JIAN WANG,<sup>b,l</sup> XINGANG LI,<sup>a,b</sup> SHILEI NI<sup>l</sup> 

**Key Words.** Melatonin • Neural stem cells • Autophagy • Hyperglycemia • Proliferation • Differentiation

### ABSTRACT

Dysfunction of neural stem cells (NSCs) has been linked to fetal neuropathy, one of the most devastating complications of gestational diabetes. Several studies have demonstrated that melatonin (Mel) exerted neuroprotective actions in various stresses. However, the role of autophagy and the involvement of Mel in NSCs in hyperglycemia (HG) have not yet been fully established. Here, we found that HG increased autophagy and autophagic flux of NSCs as evidenced by increasing LC3B II/I ratio, Beclin-1 expression, and autophagosomes. Moreover, Mel enhanced NSCs proliferation and self-renewal in HG with decreasing autophagy and activated mTOR signaling. Consistently, inhibition of autophagy by 3-Methyladenine (3-Ma) could assist Mel effects above, and induction of autophagy by Rapamycin (Rapa) could diminish Mel effects. Remarkably, HG induced premature differentiation of NSCs into neurons (Map2 positive cells) and astrocytes (GFAP positive cells). Furthermore, Mel diminished HG-induced premature differentiation and assisted NSCs in HG differentiation as that in normal condition. Coincidentally, inhibiting of NSCs autophagy by 3-Ma assisted Mel to modulate differentiation. However, increasing NSCs autophagy by Rapa disturbed the Mel effects and retarded NSCs differentiation. These findings suggested that Mel supplementation could contribute to mimicking normal NSCs proliferation and differentiation in fetal central nervous system by inhibiting autophagy in the context of gestational diabetes. *STEM CELLS* 2019;37:504–515

### SIGNIFICANCE STATEMENT

Neural stem cells play important roles in fetal neurodevelopment. The incidences of gestational diabetes are rising in the world and prevention of fetal neuropathy in gestational diabetes mellitus (GDM) needs to be deeply explored. In addition, autophagy of NSCs in HG is still unclear. Here, it is reported that HG inhibits proliferation and induces premature differentiation of NSCs by promoting autophagy and autophagic flux. The naturally occurring hormone melatonin (Mel) antagonized HG-mediated effects and maintained normal proliferation and differentiation in NSCs by modulating autophagy, which protected NSCs mainly by downregulating Beclin-1 and up modulating mTORC1 signaling. This work indicates that Mel could be used as a potential drug to aid in fetal central nervous system (CNS) development in GDM patients.

### INTRODUCTION

Gestational diabetes mellitus (GDM) accounts for 3%–5% of all pregnancies [1]. GDM imposes a substantial economic burden on both affected patients and society in general because it is highly related to malformations and maternal health complications. Central nervous system (CNS) development is especially vulnerable to GDM [2]. Several studies on offspring of mothers with GDM show higher rates of gross and fine motor abnormalities [3], attention deficit hyperactivity disorder [4], learning difficulties [4], and

autism spectrum disorder [5]. Neurodevelopment disorders [6] or neural congenital malformations [7] have been found to be due to an imbalance between proliferation and differentiation of neural stem cells (NSCs).

The cellular process of autophagy has been shown to play an important role in neural development [8]. Inhibition of autophagy has been directly linked to uncontrolled proliferation and excessive apoptosis in the development of the nervous system [9]. Autophagy, or “self-eating,” is related to mechanisms of lysosome-dependent degradation of intracellular

components during stress. Upon activation of autophagy, focal degradation of cytoplasmic areas is sequestered by a membrane structure, which is known as a phagophore. The phagophore expands and matures into an intact double-membrane structure termed an autophagosome. The engulfed materials are degraded when autophagosomes fuse with lysosomes [10]. Autophagic flux is the process of transitioning from phagophore to degradation of the contents. Several proteins, including microtubule-associated protein light chain 3 B (LC3B), p62/SQSTM1, and Beclin 1 have been implicated in the process of autophagy and are used as markers for the activation of the process. LC3B is the most widely used autophagic marker, and is located both inner and outer membranes of autophagosomes. Autophagy increases the conversion of LC3B I into LC3B II, which is degraded through lysosomal turnover [10]. Beclin-1 is an autophagy initiated protein. Accumulation of LC3B II is thus used as a marker for autophagy. p62/SQSTM1 possesses LC3-interacting region and serves as a signaling hub of autophagy. p62 is degraded through the process of autophagy, therefore its degradation can serve as a marker of autophagic clearance [11]. Increases in Beclin-1, an autophagy initiation protein, also accompany activation of the process, and the protein has been directly linked to neurogenesis. NSCs derived from Beclin-1 heterozygosis caused reduction of proliferating cells and differentiating immature neurons [12]. Finally, the mechanistic target of rapamycin (mTOR) pathway is a chief regulator of autophagy, which plays important role in proliferation and differentiation of NSCs. Type I mTOR complex (mTORC1) have different effects on stem cells differentiation at various levels. During undifferentiated stages, mTORC1/p70S6K activity is maintained at lower levels. Once NSCs begin to differentiate, mTORC1/p70S6K mediated protein translation increases [13]. Autophagy function requires more research, especially in regard to pathologies.

Clinical research has shown that high-risk pregnant women (those with gestational diabetes and hypertension) also suffer from poor quality sleep [14]. Ten genome-wide association scans involving 36,610 Europeans showed that variants in the gene encoding the melatonin (Mel) receptor 1b were associated with disruption of normal glucose homeostasis [15]. This finding indicated that Mel deficiency may be involved in normal glucose homeostasis. Mel is the "hormone of darkness" that is secreted mainly by the pineal gland, and is an indoleamine with the chemical name N-acetyl-5-methoxytryptamine. Its primary biological function is as an antioxidant, which protects the cells from toxic, free radical damage [16]. Mel obtained additional biological functions with the evolution of animals, including modulating the circadian timing system [17]. Mel has also been implicated in neuroprotective effects in many CNS diseases, such as stroke, Parkinson's and Huntington's disease [18–20]. More recently, Mel was shown to prevent neural tube defects in the offspring of diabetic pregnancy by inhibiting the cellular process of apoptosis [7]. However, the effect of Mel on autophagy in NSCs exposed to hyperglycemia (HG) has not been widely investigated.

This study aimed to explore the role of autophagy in NSCs exposed to HG and Mel as a putative neuroprotective agent *in vitro* and *in vivo*. HG damaged NSCs proliferation and enhanced premature differentiation of NSCs into neurons and astrocytes. Mel prevented HG effects on NSCs in proliferation and differentiation though inhibition of autophagy, and the

mTOR signaling participated in this process. Furthermore, inhibition of NSCs autophagy by 3-Ma assisted Mel to modulate differentiation. Interestingly, increasing NSCs autophagy by Rapa shows that Mel affects and retards NSCs differentiation. Taken together, this work indicates that Mel could be used as a potential drug in the clinical management of GDM patients to promote fetal CNS development.

## MATERIALS AND METHODS

### Ethics Statement

All procedures were performed in accordance with the International Guiding Principles for Animal Research, as stipulated by the World Health Organization (1985) and adopted by the Laboratory Animal Center at Shandong University.

### Chemicals

Melatonin, 3-methyladenine, rapamycin, poly-L-lysine hydrobromide (PLL), D-(+) glucose and streptozocin were purchased from Sigma-Aldrich (St. Louis, MO).

### Cell Culture

NSCs were prepared from the cerebral cortex of Kunming mice (obtained from the Animal Resource Center, University of Shandong, Jinan, China) at embryonic day 12.5 (E12.5) as previously described [20]. Briefly, we separated the telencephalons from E12.5 mice. Brain tissues were dissected and mechanically dissociated in the serum-free neurosphere culture medium DMEM: F12 (1:1; Gibco, Gaithersburg, MD). For proliferation, the proliferation medium was supplemented with 20 ng/ml basic fibroblast growth factor (bFGF; R&D; Minneapolis, MN), 2% B27 (Gibco), 100 U/ml penicillin, 100 µg/ml streptomycin, and 250 ng/ml amphotericin B. NSCs were incubated at 37°C in a humidified atmosphere of 5% CO<sub>2</sub> and 95% air. NSCs were cultured overnight and the culture bottles were changed to purify the primary cells on the second day. After 3 days, the cells proliferated and formed primary neurospheres (approximately 30–50 µm in diameter). Neurospheres were harvested by centrifugation, and dissociated mechanically into small neurospheres and single cells, which were replated in the medium.

To examine the proliferation of NSCs, the dissociated NSCs were cultured in proliferation medium. For differentiation of NSCs, neurospheres were transferred into differentiation medium, containing 2% fetal bovine serum (FBS, Gibco) without bFGF and B27.

### Cell Viability Assays

Indirect counting of viable cells was performed with the Cell Counting Kit-8 (CCK-8; Dojindo; Kumamoto, Japan) assay. NSCs were seeded into 96-well culture plates (Corning; Oneonta, NY) at an optimal density of  $5-8 \times 10^4$  cells per milliliter in 150 µl of proliferation culture medium per well, and were cultured overnight. Then culture medium was changed, and reagents were added to examine NSCs response. After 24 hours, the medium was replaced by the medium (100 µl) containing CCK-8 reagent (10 µl). NSCs were incubated at 37°C for 4 hours. The optical density of each sample was then measured in a multi-well spectrophotometer at 450 nm referenced to a wavelength of 630 nm. Experiments were performed in quadruplicate.

### 5-Ethynyl-2'-Deoxyuridine Labeling and Immunostaining

Cell proliferation was measured using the 5-ethynyl-2'-deoxyuridine (EdU; Guangzhou Ribobio, Co.; Guangzhou, Guangdong, China) assay. NSCs were seeded into the 96-well plates overnight and were treated with Mel, 3-Ma or Rapa for 24 hours. EdU (50  $\mu$ M) was added, and cells were incubated for 4 hours. Cells were fixed in 4% paraformaldehyde (PFA) for 20 minutes and permeabilized with 0.3% Triton X-100 for 20 minutes. Cells were incubated with the Apollo reaction medium, a reaction cocktail containing buffer, Alexa Fluor azide and  $\text{CuSO}_4$ , for 30 minutes at room temperature. The Apollo reaction mixture was removed, and cells were rinsed once with phosphate-buffered saline (PBS) for 5 minutes. Hoechst33342 were added for 30 minutes to highlight nuclei. The cells were rinsed with PBS. The assay was performed according to the manufacturer's instructions. Images were obtained under fluorescence microscopy.

### Immunocytochemistry

NSCs were plated on coverslips in 24-well plates (15  $\times$  10<sup>4</sup> cells per well) coated with PLL. After Mel, 3-Ma or Rapa treatments, the medium was removed. Cells were fixed in 4% PFA for 20 minutes and rinsed with PBS. The cells were permeabilized with 0.3% Triton X-100 for 20 minutes at room temperature. Subsequently, cells were blocked with 3% FBS for 30 minutes, and incubated with primary antibodies at 4°C overnight: anti-Ki 67 (1:100, rabbit polyclonal; Abcam; Cambridge, MA), anti-LC3B (1:100, rabbit polyclonal; Cell Signaling Technology; Beverly, MA), anti-Map2 (1:100, rabbit polyclonal; Boster; Wuhan, Hubei, China), and anti-GFAP (1:100, mouse polyclonal; Boster). The second antibodies (1:100, DyLight 488 or 594 conjugated goat anti-mouse or rabbit IgG [H+L]; Abbkine) were incubated with the cells for 1 hour, and nuclei were counterstained with 4',6'-diamidino-2-phenylindole (DAPI; Boster). Images were obtained and analyzed using fluorescence microscopy (IX71; Olympus; Tokyo, Japan).

### Western Blotting Analysis

Western blotting was performed as described previously [7, 20]. Protein concentrations were assayed colorimetrically. Proteins were loaded onto a 10% or 15% gradient polyacrylamide gel, and electrophoretically transferred to a polyvinylidene difluoride membrane. Membranes were blocked with 5% dried milk and subsequently incubated with primary antibody overnight. The following antibodies were used: p-S6k, S6k, LC3B (1:1,000; rabbit polyclonal; Cell Signaling Technology), Beclin-1 (1:1,000; rabbit polyclonal; Boster), and  $\beta$ -actin (1:1,000; mouse monoclonal; Boster). Secondary antibodies were horseradish peroxidase conjugated to goat anti-rabbit IgG or anti-mouse IgG (1:5,000; mouse monoclonal; Boster). Secondary antibodies were incubated with membrane for 1 hour at 37°C. The immunoreactive bands were visualized by the ECL detection kit (Millipore; Burlington, MA). The intensity of the bands was quantified with the Image Processing and Analysis in Java software (ImageJ, Media, and NIH).

### RNA Extraction and Real-Time PCR

Total RNA was isolated from NSCs (1  $\times$  10<sup>6</sup> cells) using the TRIZOL (Invitrogen, Carlsbad, CA) method. RNA was reverse transcribed

and purified using the PrimeScript RT reagent Kit with gDNA Eraser (Takara; Kusatsu, Shiga, Japan). The PCR primers used were the following: Map2 mouse forward, 5'-TCCTCCCTATAAGTCT GG-3'; reverse, 5'-GCATCTCAACCTCGGCTA-3'; GFAP mouse forward, 5'-CTACATCGAGAAGGTCCGCT-3'; reverse, 5'-CCTGTGCAAA GTTGCCCTC-3' and  $\beta$ -actin primer: forward, 5'-AGATGTGGATCA GCAAGCAG-3'; reverse, 5'-GCGCAAGTTAGTTTTGTCA-3'. RT-PCR for Map2, GFAP, and  $\beta$ -actin were performed using the SYBR Premix Ex Taq (Takara). All processes were performed according to the manufacturer instructions.

### Ultrastructure Analysis with Transmission Electron Microscopy

A transmission electron microscope (TEM) was used for ultrastructural analysis of NSCs and brain tissues. Briefly, NSCs or fresh brain tissues were fixed with 3% glutaraldehyde at 4°C for 24 hours. After fixation, tissue or NSCs were rinsed twice in PBS immediately, postfixed in 1% osmium tetroxide, and then dehydrated in a graded ethanol series. After dehydration, tissue was embedded in EPON (EMS, Fort Washington, PA). Ultrathin sections (50 nm) were cut with an ultramicrotome (Leica UC-6, Leica Microsystems, Nussloch, Germany), stained with uranyl acetate and lead citrate, and examined via TEM (JEM-1200EX, JEOL Transmission Electron Microscope, Tokyo, Japan) at an accelerating voltage of 80 kV.

### Mouse Experiments

Kunming mice (8 weeks old) were randomly divided into 3 groups, containing 8 mice per group. Diabetes mellitus mice were induced by intraperitoneal (i.p.) injection of streptozotocin (STZ, 75 mg/kg) for 3 consecutive days. After 5 days, mice with blood glucose levels exceeding 16.7 mM (300 mg/dl) were defined as diabetic mice. Female mice were fertilized with healthy male Kunming mice in one cage. The emergence of a copulation plug was designated as embryonic day E0.5. Pregnant mice were given 10 mg/kg Mel (dissolved in ethanol, and diluted with Saline) until sacrificed. Mice from the control (Con) and HG groups were injected with DMSO and saline in the same manner. All mice were maintained under the same breeding conditions. At E11.5 and 17.5 embryos were collected by cesarean section. Three to five babies were randomly chosen from for further testing, and only 1 baby was chosen from same dam for same testing. The brains of the embryos were fixed in 4% PFA in PBS at 4°C overnight and dehydrated with 20% and 30% sucrose in PFA. Brains were sections (6  $\mu$ m) using a Cryostat Microtome (Leica CM 3050; Leica Microsystems, Nussloch, Germany).

### Statistical Analysis

Data are presented as the mean  $\pm$  SD for continuous variables and as numbers or percentages for categorical variables. Statistical significance was determined using the *t* test in 2 groups, and one-way analysis of variance was performed to compare data (for  $\geq$ 3 groups), using Dunnett's multiple comparison post hoc test. A *p* value  $<$ .05 was considered to be significant. All the data analysis and expression was performed using Statistical Package for the Social Sciences 20.0 for Windows (SPSS, Inc.; Chicago, IL) and Graphpad Prism7.0 (GraphPad Software; La Jolla, CA).

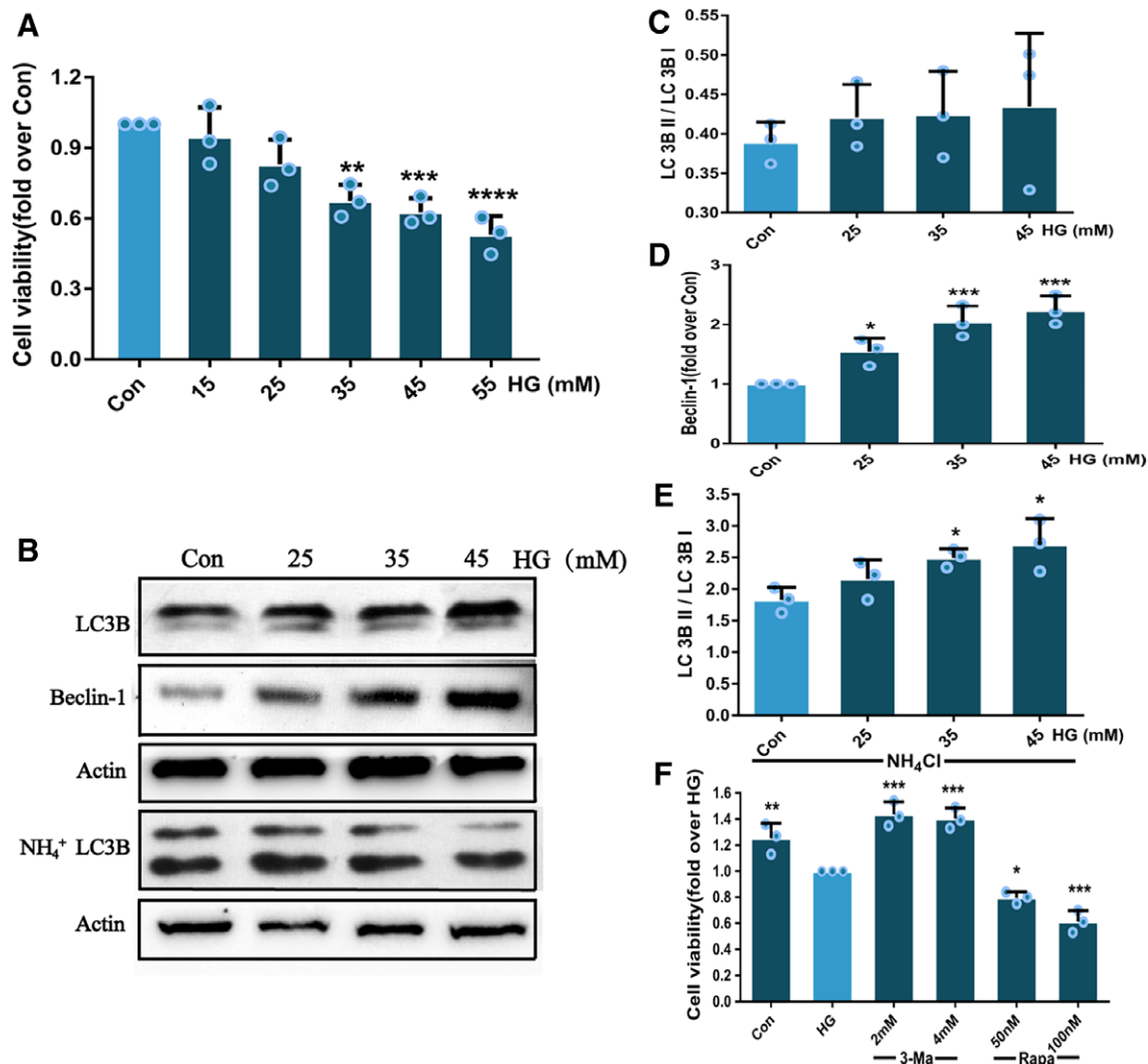


**Figure 1.** Increased autophagy mediates reduced viability of neural stem cell (NSC) in hyperglycemia. **(A):** NSCs were treated with different concentrations of D-glucose for 24 hours, and cell viability was determined by CCK-8 assay. **(B):** Western blotting analysis showed LC3B and Beclin-1 expression in NSCs exposed to different concentrations of glucose for 24 hours. The second LC3B was detected under the same conditions, with 4 hours NH<sub>4</sub><sup>+</sup> treatment before collecting the protein samples. **(C–E):** Column graphs show the Western blotting results, the ratio between LC3B II and LC3B I, and Beclin-1 protein expression. Values are compared with con. **(F):** The viabilities of NSCs were treated with autophagy inhibitor and inducer in HG for 24 hours. Values were compared with hyperglycemia (HG). All experiments were performed three times, and the bulbs represent the results from each experiment. Values are mean ± SD. \*,  $p < .05$ ; \*\*,  $p < .01$ ; \*\*\*,  $p < .001$ ; \*\*\*\*,  $p < .0001$ .

## RESULTS

### Increased Autophagy Mediates Reduced Viability of NSC in HG

NSCs were cultured in the medium with increasing concentrations of D-(+)-glucose (15, 25, 35, 45, and 55 mM). The NSCs viability was assessed by CCK-8 assay. The results showed that treatment with increasing concentrations of glucose for 24 hours repressed the cell viability in a dose-dependent manner (Fig. 1A). When concentration of glucose was over 35 mM, it exhibited decreased cell viability.

We then examined whether HG might stimulate autophagy in NSCs. Protein lysates were prepared from NSCs treated with increasing concentrations of glucose (25–45 mM), and protein marker for autophagy, LC3B and Beclin-1, were examined by Western blot (Fig. 1B). The ratio of LC3B II/I did not change

significantly in NSCs under varying HG conditions (Fig. 1C). However, Beclin-1 protein levels were significantly increased and p62 was decreased (Supporting Information), indicating that autophagy might be enhanced (Fig. 1D). Therefore, we further investigated the LC3B II/I ratio by treating NSCs with inhibitors of autophagic flux. NSCs were first treated with the H<sup>+</sup>-ATPase inhibitor, Bafilomycin A1 (BAF A1, 100 nM) which blocks fusion of autophagosomes and lysosomes, and thus inhibited degradation of LC3B II by the lysosomal enzymes [21]. However, in our system, BAF A1 did not efficiently block autophagic flux. Thus, we used a second lysosomotropic agent, NH<sub>4</sub>Cl, which penetrates acidic compartments and raises the pH in lysosomes to inhibit lysosomal degradation of the LC3B II [21–23]. NSCs were treated with 10 mM NH<sub>4</sub>Cl for 4 hours before collecting samples. Importantly, the concentration of NH<sub>4</sub>Cl at 10 mM did not change medium pH to disturb cellular

metabolism. The Western blotting results revealed that a trend for an increasing LC3B II/I ratio was observed in HG-treated NSCs exposed to  $\text{NH}_4\text{Cl}$  (Fig. 1E). These results suggested that autophagic flux, from the process of phagophore formation to fusion with lysosomal system and degradation, was enhanced when cells were incubated under HG conditions.

Next, we assessed the role of NSCs autophagy in HG (35 mM). To test this, we used the autophagic inhibitor (3-Ma) or the autophagic inducer (Rapa) to treat NSCs under HG conditions. The results showed that inhibiting autophagy by 3-Ma (2 and 4 mM) significantly promoted cell viability and inducing autophagy by Rapa (50 and 100 nM) exhibited opposite results, suggested that decreased NSCs viability in HG was due to increased autophagy (Fig. 1F). Furthermore, 35 mM  $\text{D-glucose}$ , 2 mM 3-Ma and 50 nM Rapa were sufficient to yield the appropriate response in NSCs. These concentrations of these reagents were therefore applied to NSCs in subsequent experiments unless otherwise stated.

### Melatonin Enhances NSCs Viability in HG

We next investigated the viability of NSCs in 35 mM HG after exposure to various concentrations of Mel (10 nM, 100 nM, 1  $\mu\text{M}$ , and 10  $\mu\text{M}$ ). Cell viability was enhanced in the presence of Mel at dosage ranges from 10 nM to 1  $\mu\text{M}$ , but further reduced at Mel concentrations  $>1 \mu\text{M}$  (Fig. 2A). Because 100 nM Mel yielded the optimal effects of cell viability (Fig. 2A), we used this concentration in subsequent experiments unless otherwise stated.

### Mel Inhibits Autophagy of NSCs in HG

Mel has been shown to both promote and inhibit autophagy, but the effects are dependent on different cell types and different pathologies [24–28]. To determine the influence of Mel on autophagy in NSCs, the expression levels of LC3B, Beclin-1, and mTOR signaling downstream substance p-S6k were examined. A significant LC3B result could not be detected in HG, so  $\text{NH}_4\text{Cl}$  was added to block autophagic flux. The results showed that HG improved LC3B II/I ratio and Mel counteracted upregulation of LC3B II/I ratio (Fig. 2B, 2C). HG markedly increased the level of Beclin-1 and reduced p-S6k in NSCs. Under HG condition, in the presence of Mel, autophagy appeared to be attenuated in NSCs, because Beclin-1 was reduced and p-S6k was increased (Fig. 2B, 2D, 2E). The autophagy activator Rapa inhibited the effect of Mel on NSCs; p-S6k expression was reduced (Fig. 2B, 2E). Finally, the autophagy inhibitor 3-Ma enhanced the effect of the hormone on NSC; the level of p-S6k was increased in HG.

Immunocytochemistry was used to confirm the results for LC3B. For these experiments, cells were treated as indicated for 24 hours followed by exposure to  $\text{NH}_4\text{Cl}$  for 4 hours before fixation of cells for immunocytochemistry. Consistent with the Western blotting results, the immunofluorescence analysis of LC3B showed that HG increased the number of LC3B-positive cells and Mel blocked HG-mediated effects. Rapa inhibited the Mel effects and led to the greatest number of LC3B-positive cells and 3-Ma supplement assisted Mel effects and decreased LC3B-positive cells (Fig. 2F, 2G).

Finally, we used transmission electron microscopy, the gold standard for monitoring autophagy, to confirm autophagy in NSCs. HG induced autophagosomes and mitochondrial swelling

in NSCs. Mel antagonized these changes in NSCs; the number of autophagosomes was decreased and the morphology of mitochondrial body remained normal (Fig. 2H, 2I). All together, these results suggested that Mel inhibited autophagy in NSCs in HG conditions.

### Melatonin Promotes NSCs Proliferation and Self-Renewal of NSCs in HG

To assess the effect of Mel on cell proliferation, we performed EdU staining. HG led to decreased proliferation relative to the Con, and Mel could obviously promote cell proliferation in HG (Fig. 3A). Furthermore, inhibiting autophagy by 3-Ma together with Mel in HG contributed to cell proliferation, and increasing autophagy by Rapa inhibited the Mel protective effects.

We next performed the neurosphere formation test, neurospheres formed under all culture conditions, there were measurable differences in the size and the numbers of the spheres formed. The number of neurospheres formed was reduced in HG-treated group relative to Con group (Fig. 3B). More importantly, Mel supplementation opposed HG-mediated effects (Fig. 3B). Consistently, increasing autophagy by Rapa blocked Mel effect on neurospheres formation. On the contrary, inhibition of autophagy by 3-Ma assisted Mel effect on neurospheres formation (Fig. 3B). Specifically, the diameters of spheres were larger in the Mel group relative to the HG group, and addition of the autophagy inhibitor 3-Ma led to further increases in the diameter of these spheres. However, this difference between Mel group and 3-Ma group was not statistically significant. In contrast, addition of the autophagy activator Rapa decreased the diameter of spheres (Fig. 3B).

These results indicated that Mel could protect NSCs proliferation and self-renew abilities from HG through inhibition of autophagy.

### Melatonin Inhibits Premature Differentiation of NSCs in HG

For cell differentiation analysis, we assessed protein and mRNA levels of astrocyte marker GFAP and neuron marker Map2 using qPCR and immunocytochemistry at 5 days. The number of Map2-positive and GFAP-positive cells increased in the HG group compared to that in the Con group, indicating that HG triggered NSCs premature differentiation. More importantly, HG-induced premature differentiation could be diminished by Mel (Fig. 4A, 4B). Interestingly, the autophagy inducer Rapa as well as 3-Ma led to suppression of Map2- and GFAP-positive cells among HG-treated NSCs in the presence of Mel (Fig. 4A, 4B). RNA levels of Map2 and GFAP were increased in HG compared with Con (Fig. 4C). However, Map2 and GFAP mRNAs did not increase over controls under HG treatment in the presence of Mel. Again, Map2 and GFAP were suppressed in NSC under HG treatment by Rapa as well as 3-Ma in the presence of Mel (Fig. 4C). In fact, Rapa treatment led to significantly decreased Map2 and GFAP mRNA levels compared to controls (Fig. 4C). Thus, increased autophagy induced by Rapa may impair differentiation of NSCs. Taken together, Mel shows good potential to diminish premature differentiation of neurons and astrocytes, and mimicked the NSCs differentiation under normal condition.

### Melatonin Antagonizes HG In Vivo

Mice were randomly divided into 3 groups, Con, HG and Mel treatment groups. Fasting blood glucose levels were not

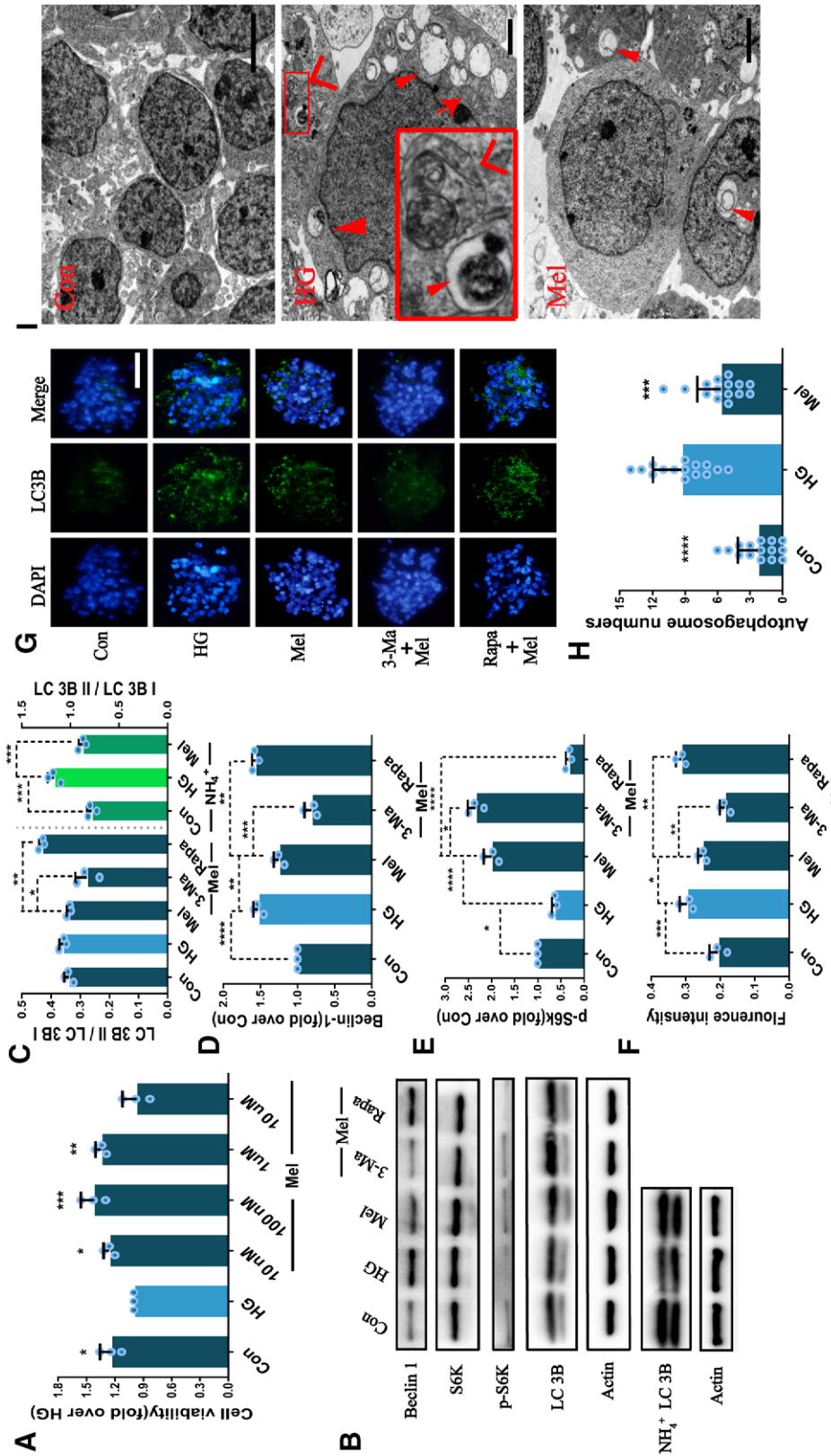


**Figure 2.** Melatonin enhances neural stem cells (NSCs) viability by inhibiting autophagy in hyperglycemia. **(A):** NSCs were treated with various dosage of Mel for 24 hours, and cell viability was determined by the CCK-8 assay. All groups were compared with the hyperglycemia (HG) group. **(B–E):** Western blotting analysis of NSCs treatment with agents for 24 hours. **(F, G):** Immunofluorescent detection of LC 3B expression in NSCs when cells were treated with different agents in HG for 24 hours. Scale bar: 20 μm (×40). **(H, I):** Transmission electron microscopy analysis of NSCs exposed to HG. Con group had few autophagosomes. Scale bar: 2 μm (×7,500). HG group: triangular arrowhead indicated an early autophagosome, which contained cell organelles. Arrow indicated swelling mitochondria and arrowhead shown late autophagosomes. Scale bar: 1 μm (×10,000). Mel: arrowhead showed an autophagosome. Scale bar: 1 μm (×10,000). Column chart showed the quantity of autophagosomes per cell. All experiments were performed three times; the results represent the results from each experiment. Values are mean ± SD. \*,  $p < .05$ ; \*\*,  $p < .01$ ; \*\*\*,  $p < .001$ ; \*\*\*\*,  $p < .0001$ .

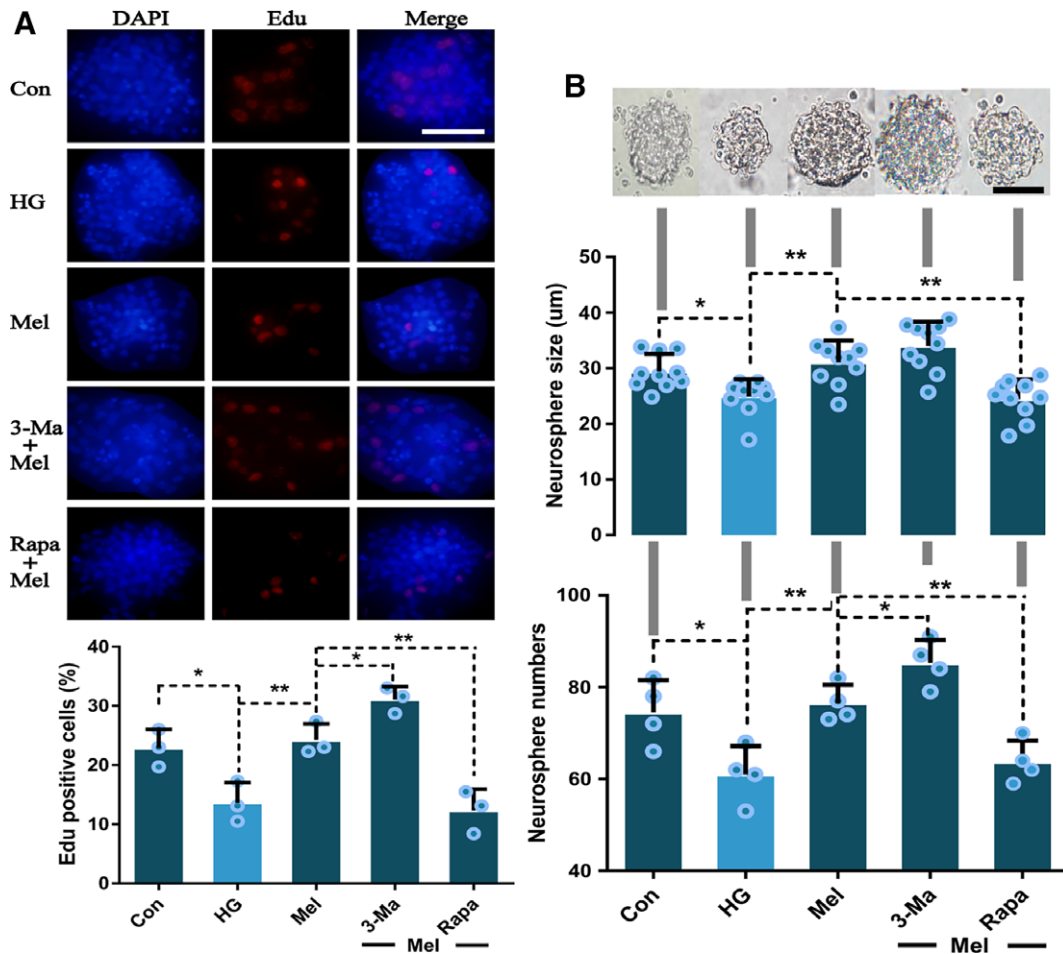


**Figure 3.** Melatonin contributes to proliferation and neurosphere formation. **(A):** Immunofluorescence images showed 5-ethynyl-2'-deoxyuridine (EdU)-positive cells. And the column graphs represented the percentage of EdU. **(B):** The numbers and diameters of neurospheres were measured. Representatives of neurospheres images are shown at the top. The bulbs represent the results from each experiment. Scale bar represents: 20 µm (×40). Values are mean ± SD. \*,  $p < .05$ ; \*\*,  $p < .01$ .

significantly different among groups (Con  $4.45 \pm 0.9$ , HG  $4.57 \pm 0.87$ , and Mel  $4.53 \pm 0.76$  mM). Diabetes mellitus was induced in mice in HG and Mel groups though treatment with STZ. The mice in the Mel group were treated with Mel every day (10 mg/kg intraperitoneal injection) from the day they were mated to the day of sacrifice. And Mel group showed no difference in random blood glucose levels compared with HG group (Con  $6.3 \pm 1.2$ , HG  $18.4 \pm 3.4$ , and Mel  $17.5 \pm 4.1$  mM; Fig. 5A).

We chose 11.5 days pregnant mice to stain brain slices with Ki67 and LC3B. The HG group had fewer Ki67-positive cells than the Con group, indicating that HG suppressed cell proliferation. Mel supplement markedly diminished HG-mediated inhibition of cell proliferation by increasing Ki67-positive cells (Fig. 5B, 5C). In regard to cell autophagy analysis, More LC3B-positive cells were detected in brain sections from the HG group than that in the Con group, which was consistent with increased autophagy in NSCs in vitro. However, under Mel treatment, the number of LC3B-positive cells in HG animals was again comparable to controls (Fig. 5D, 5E).

We next stained E17.5 mice's brain slices with Map2 and GFAP to investigate cell differentiation. Because neurogenesis and gliogenesis reach their peaks before and after birth, respectively,

GDM influences neurogenesis more than gliogenesis [29]. We focused on the cortical region, which contains mainly neurons. Here, the HG mice exhibited a significantly greater area of Map2 expression than controls. However, Mel treatment significantly reduced the area of Map2 expression induced by HG (Fig. 6). Similar results were found for GFAP expression (Fig. 6).

Finally, we used TEM to detect autophagy in brain tissues from the treated animals. We observed autophagosomes, which had two parallel membrane bilayers and contained mitochondria, ribosomes and endoplasmic reticulum (Fig. 7). HG treatment enhanced the formation of autophagosomes compared to the Con group, and led to mitochondrial swelling. Such effects were diminished in the presence of Mel (Fig. 7).

## DISCUSSION

Identifying the molecular basis for the association between GDM and neurological abnormalities in offspring might lead to improvements in the clinical management of these patients. Here, we found HG increased autophagic flux and decreased proliferation of NSCs. Remarkably, Mel promoted viability and proliferation of NSCs exposed to HG. As it has previously been

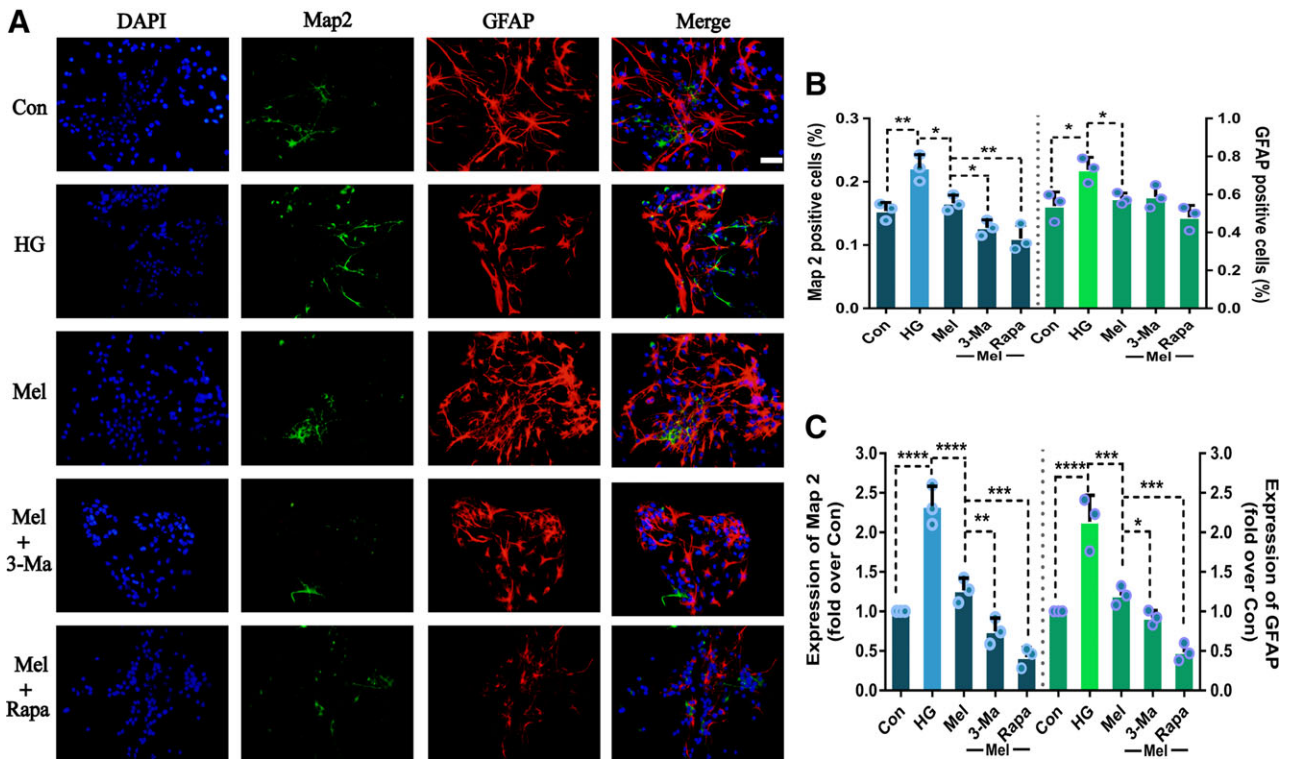


**Figure 4.** Melatonin inhibits premature differentiation of neural stem cells (NSCs) in hyperglycemia. **(A, B):** NSCs were cultured in 2% FBS with different agents for 5 days. Immunofluorescence images showed the number of Map2 (green) and GFAP (red)-positive cells. Scale bar: 40  $\mu$ m ( $\times$ 40). **(C):** qPCR analysis showed expression of Map2 and GFAP mRNA. The bulbs represent the results from each experiment. Values are mean  $\pm$  SD. \*,  $p < .05$ ; \*\*,  $p < .01$ ; \*\*\*,  $p < .001$ ; \*\*\*\*,  $p < .0001$ .

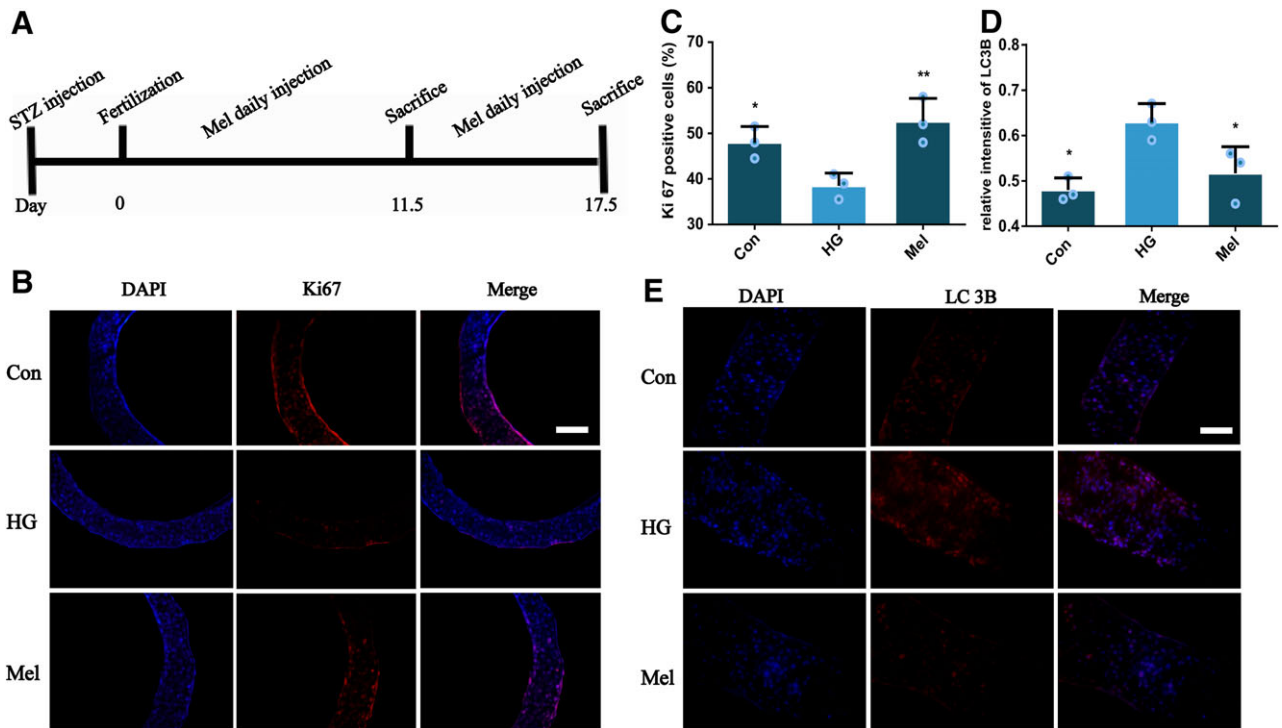


**Figure 5.** Melatonin enhanced proliferation and decreased autophagy of neural stem cells (NSCs) in vivo. **(A):** Illustration of the animal study profile. **(B, C):** The neural tubes were stained with Ki67 in the presence or absence of melatonin (10 mg/kg per day) treatment at E11.5. **(D, E):** The neural tube was stained by LC3B. Scale bar: 40  $\mu$ m ( $\times$ 40). Values are mean  $\pm$  SD. \*,  $p < .05$ ; \*\*,  $p < .01$ ; \*\*\*,  $p < .001$  compared to the hyperglycemia group.

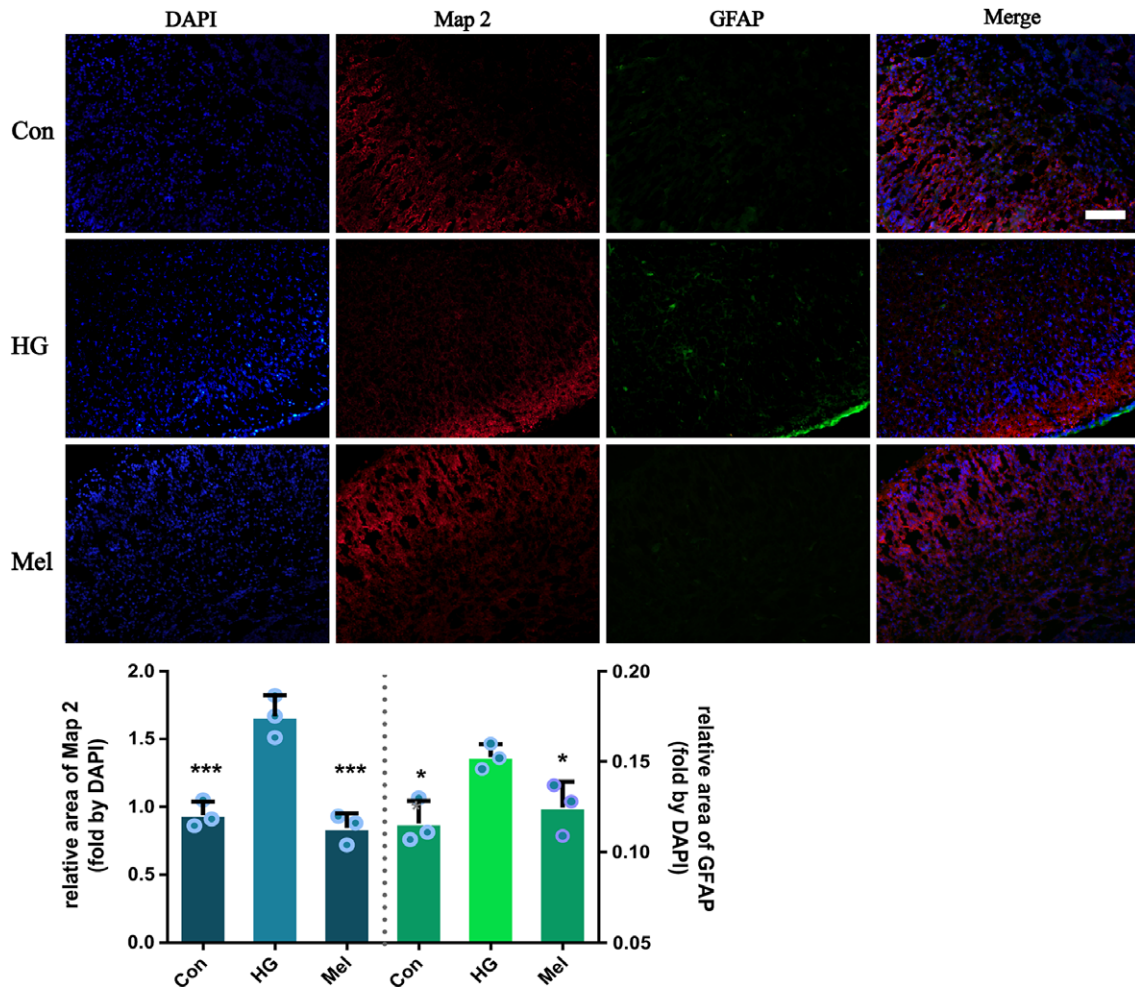


**Figure 6.** Mel decreased premature differentiation of neural stem cells in vivo. Immunofluorescence image showed double staining of Map2 (red) and GFAP (green) within the E17.5 cortex of mice. Scale bar: 100  $\mu$ m ( $\times$ 20). Values are mean  $\pm$  SD. \*,  $p < .05$ ; \*\*,  $p < .01$ ; \*\*\*,  $p < .001$  compared to the HG group.

reported that Mel also prevents NSCs in HG from apoptosis [7], Mel could protect NSCs from programmed cell death, including apoptosis and autophagy. Therefore, Mel may be an ideal drug to use in pregnant women with GDM to prevent NSCs from death in fetuses.

Recent studies demonstrated that the autophagy related genes including Ambra 1, Atg5, and Beclin-1 contribute to neurogenesis and differentiation. Autophagy may play an important role in the development of NSCs under physiological condition [12, 30]. NSCs differentiation fate was dependent on specific pathology as well as autophagic conditions [31–34] and even on different concentration of Mel [35]. Here, we found that HG triggered early differentiation of NSCs into neurons and astrocytes, whereas Mel effectively opposed HG-mediated differentiation, especially neurogenesis. Neurogenesis peaks in the pregnancy period at E14 in mice, whereas astrocytogenesis occurs at postnatal day (P)-2 and oligodendrocytogenesis at P14 [29]. Thus, this is the reason why GDM mainly influenced neurogenesis and Mel inhibited HG-induced NSCs differentiation into neuron phenotype in the present study. Interestingly, Mel with Rapa inhibited the NSCs differentiation in HG, and the results were inconsistent that increasing autophagy by HG caused NSCs premature differentiation. The

reason for this phenomenon might be the different level of autophagy induced by HG or Rapa. The further study needed to be done to explain this phenomenon. Yang et al. have demonstrated that glucose at a concentration of 20 mM inhibited differentiation of embryonic stem cells (E14 mouse ESC line) into neurons [36]. In contrast, we used 35 mM glucose that led to premature of NSCs into neurons. Therefore, these opposite results may be due to different stem cell types used and different high glucose concentrations. Accumulation of morphologically abnormal mitochondria was also detected in NSCs after HG treatment in vivo and in vitro. Thus, changes in mitochondrial morphology might be partially responsible for premature differentiation. Khacho et al. discovered that manipulation of the mitochondrial structure could promote NSCs differentiation by driving the production of reactive oxygen species (ROS) [37]. Furthermore, Yang et al. showed that a decrease in the level of glyoxalase 1, a detoxifying enzyme, could induce premature differentiation of neural precursor cells in GDM mice [38]. Taking together, premature differentiation of NSCs caused by maternal diabetes might involve many pathological factors, including abnormal accumulation of mitochondria, HG, ROS, and methylglyoxal.

Several of our results indicated that HG induced autophagy of NSCs, including increases in the number of autophagosomes

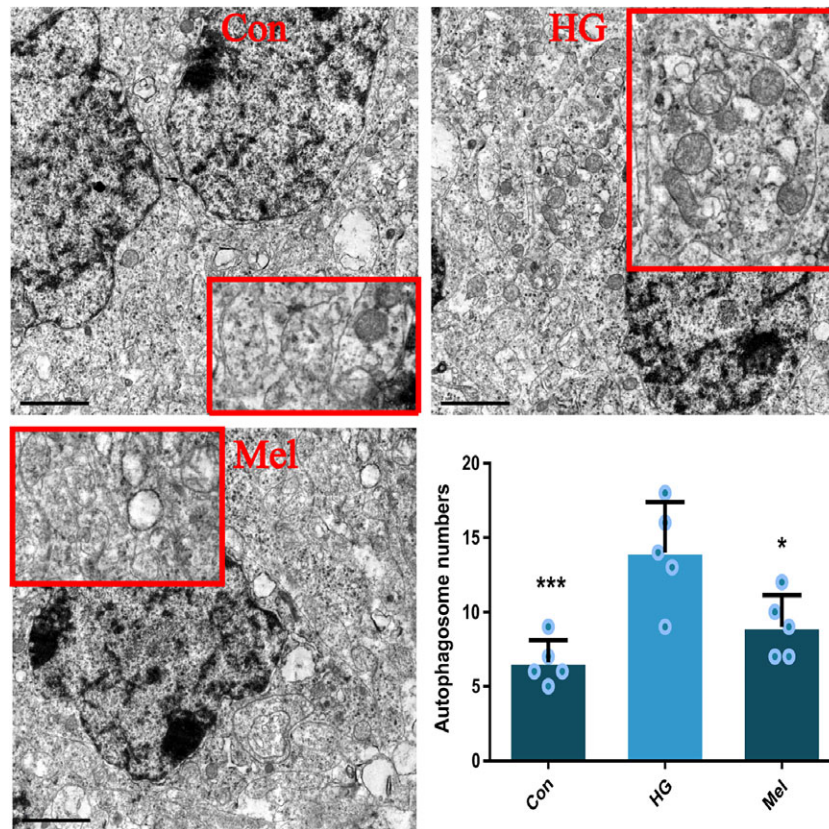


**Figure 7.** Ultrastructure of autophagy in brain tissues. Transmission electron microscopy images showed the autophagosomes and swelling mitochondria. Column chart showed the quantity of autophagosomes per field. Values are mean  $\pm$  SD. \*,  $p < .05$ ; \*\*,  $p < .01$ ; \*\*\*,  $p < .001$  compared to the HG group. Scale bar: 2  $\mu$ m ( $\times 7,500$ ).

observed by TEM and Beclin-1 expression level. Although we initially observed no stable trend of LC3B expression in NSCs treated with different dosages of HG, we examined whether this may be due to the rapid speed of autophagosomes fusion with lysosomes, which led to more LC3B II degradation. To confirm this, we firstly blocked autophagic flux by BAF A1. However, BAF A1 failed in disrupting autophagy flux in our system, possibly due to insufficient penetration of drug into neurospheres. Therefore, we replaced BAF A1 with  $\text{NH}_4\text{Cl}$ , a lysosome inhibitor, to interrupt autophagic flux. We used 10 mM in our study, and a concentration of  $\text{NH}_4\text{Cl}$  less than 250 mM could not inhibit lysosomal function and change the medium pH [22]. In the presence of  $\text{NH}_4\text{Cl}$ , the ratio of LC3B II/I tended to increase in HG-treated NSCs. However, a recent study reported that HG inhibited E10.5 brain autophagy in vivo [39]. Our explanation for this discrepancy is as following: (a) we used NSCs mainly at E11.5 and (b) we examined the relationship between autophagy and HG in vitro and autophagic flux could be easily blocked, but autophagic flux was hardly blocked in vivo. The discrepancy was probably related to autophagy flux interference. Because of the sensitivity of NSCs to autophagy, more study methods need to be used to estimate the relationship between stress and autophagy. Studies have also reported that HG contributes to autophagy in retinal cells and placenta [40, 41]. However, HG has also been shown to impair autophagy in endothelial progenitor cells and umbilical vein endothelial cells [42, 43]. These different results indicate that modulation of autophagy is complex and possibly dependent on the tissues and the pathologic conditions.

Dysregulation of mTOR signaling underlies various brain developmental disorders, such as autism, dyslexia, epilepsy, ADHD, and mental retardation [8]. Therefore, we investigated this pathway as a potential mediator of Mel activity in NSCs. In fact, mTOR has been shown to regulated stem cells functions. Furthermore, activating mTOR signaling has been shown to contribute to proliferation of neural progenitor cells and enhance neurogenesis in aging mice [44]. In undifferentiated embryonic stem cells, p70S6k activity is maintained at low levels. Once the cells begin to differentiate, mTORC1 and p70S6K mediate protein translation increased [13]. Indeed, we demonstrated that Mel decreased autophagy by activating mTOR signaling. Interestingly, although both HG and Rapa treatment decreased mTOR activity, these treatments elicited different effects on differentiation. HG caused premature differentiation of NSCs, while Rapa treatment led to retard of differentiation. Different level of mTOR inhibition may be responsible for these differences. Thus, Mel might decrease neurogenesis and gliogenesis by activating the mTOR pathway, which could mimic the normal NSCs differentiation.

## CONCLUSION

We discovered HG reduced viability and induced premature differentiation of NSCs by increasing autophagy. However, the hormone Mel suppressed HG-induced autophagy thereby promoting NSCs proliferation and self-renewal of NSCs. In addition, NSCs were treated with Mel could diminish premature

differentiation and mimic the normal NSCs differentiation in HG. Thus, Mel is potentially an ideal supplement for GDM patients to prevent fetal neurodevelopment diseases.

#### ACKNOWLEDGMENTS

This work was supported by funding from Natural Science Foundation of China (grants 81472353 and 81402059), the Department of Science & Technology of Shandong Province (grants 2015ZDXX0801A01 and 2018GSF118094), and the Fundamental Research Funds of Shandong University (grant 2016JC019), Taishan Scholars Program of Shandong Province, China (grants ts201511093, tshw201502056, and ts20110814), the Norwegian Centre for International Cooperation in Education (SIU; grant UTF-2014/10047), The Key Research and Development Program

of Shandong Province (grant 018GSF118094), and Jinan Science and Technology Program (grant 201821049).

#### AUTHOR CONTRIBUTIONS

X.L., S.N., and Y.Z.: project conception and design, financial support, final approval of the manuscript; H.L., S.L., F.L., Y.L., and B.W.: performance of experiments; J.W., L.C., T.X., and Q.Y.: data analysis and interpretation; H.C., Y.Z., X.Z., J.W., and G.L.: data collection and manuscript revision.

#### DISCLOSURE OF POTENTIAL CONFLICTS OF INTEREST

The authors indicated no potential conflicts of interest.

#### REFERENCES

- Bellamy L, Casas JP, Hingorani AD et al. Type 2 diabetes mellitus after gestational diabetes: A systematic review and meta-analysis. *Lancet* 2009;373:1773–1779.
- Ornoy A, Reece EA, Pavlinkova G et al. Effect of maternal diabetes on the embryo, fetus, and children: Congenital anomalies, genetic and epigenetic changes and developmental outcomes. *Birth Defects Res C Embryo Today* 2015;105:53–72.
- Ornoy A, Wolf A, Ratzon N et al. Neurodevelopmental outcome at early school age of children born to mothers with gestational diabetes. *Arch Dis Child Fetal Neonatal Ed* 1999;81:F10–F14.
- Boney CM, Verma A, Tucker R et al. Metabolic syndrome in childhood: Association with birth weight, maternal obesity, and gestational diabetes mellitus. *Pediatrics* 2005;115:e290–e296.
- Lyall K, Pauls DL, Spiegelman D et al. Pregnancy complications and obstetric suboptimality in association with autism spectrum disorders in children of the Nurses' Health Study II. *Autism Res* 2012;5:21–30.
- Murai K, Sun G, Ye P et al. The TLX-miR-219 cascade regulates neural stem cell proliferation in neurodevelopment and schizophrenia iPSC model. *Nat Commun* 2016;7:10965.
- Liu S, Guo Y, Yuan Q et al. Melatonin prevents neural tube defects in the offspring of diabetic pregnancy. *J Pineal Res* 2015;59:508–517.
- Lee DY. Roles of mTOR signaling in brain development. *Exp Neurobiol* 2015;24:177–185.
- Fimia GM, Stoykova A, Romagnoli A et al. Ambra1 regulates autophagy and development of the nervous system. *Nature* 2007;447:1121–1125.
- Mizushima N. A brief history of autophagy from cell biology to physiology and disease. *Nat Cell Biol* 2018;20:521–527.
- Katsuragi Y, Ichimura Y, Komatsu M. p62/SQSTM1 functions as a signaling hub and an autophagy adaptor. *FEBS J* 2015;282:4672–4678.
- Yazdankhah M, Farioli-Vecchioli S, Tonchev AB et al. The autophagy regulators Ambra1 and Beclin 1 are required for adult neurogenesis in the brain subventricular zone. *Cell Death Dis* 2014;5:e1403.
- Easley CAT, Ben-Yehudah A, Redinger CJ et al. mTOR-mediated activation of p70 S6K induces differentiation of pluripotent human embryonic stem cells. *Cell Reprogram* 2010;12:263–273.
- Saadati F, Sehhatie Shafaei F, Mirghafourvand M. Sleep quality and its relationship with quality of life among high-risk pregnant women (gestational diabetes and hypertension). *J Maternal Fetal Neonatal Med* 2018;31(2):150–157.
- Prokopenko I, Langenberg C, Florez JC et al. Variants in MTNR1B influence fasting glucose levels. *Nat Genet* 2009;41:77–81.
- Tan DX, Manchester LC, Qin L et al. Melatonin: A mitochondrial targeting molecule involving mitochondrial protection and dynamics. *Int J Mol Sci* 2016;17:e2124.
- Schippers KJ, Nichols SA. Deep, dark secrets of melatonin in animal evolution. *Cell* 2014;159:9–10.
- Antunes Wilhelm E, Ricardo Jesse C, Folharini Bortolato C et al. Correlations between behavioural and oxidative parameters in a rat quinolinic acid model of Huntington's disease: Protective effect of melatonin. *Eur J Pharmacol* 2013;701:65–72.
- Kilic U, Yilmaz B, Reiter RJ et al. Effects of memantine and melatonin on signal transduction pathways vascular leakage and brain injury after focal cerebral ischemia in mice. *Neuroscience* 2013;237:268–276.
- Fu J, Zhao SD, Liu HJ et al. Melatonin promotes proliferation and differentiation of neural stem cells subjected to hypoxia in vitro. *J Pineal Res* 2011;51:104–112.
- Michiorri S, Gelmetti V, Giarda E et al. The Parkinson-associated protein PINK1 interacts with Beclin1 and promotes autophagy. *Cell Death Differ* 2010;17:962–974.
- Calvo-Garrido J, Carilla-Latorre S, Mesquita A et al. A proteolytic cleavage assay to monitor autophagy in *Dictyostelium discoideum*. *Autophagy* 2011;7:1063–1068.
- Castino R, Fiorentino I, Cagnin M et al. Chelation of lysosomal iron protects dopaminergic SH-SY5Y neuroblastoma cells from hydrogen peroxide toxicity by precluding autophagy and Akt dephosphorylation. *Toxicol Sci* 2011;123:523–541.
- Zhang M, Lin J, Wang S et al. Melatonin protects against diabetic cardiomyopathy through Mst1/Sirt3 signaling. *J Pineal Res*. 2017;63:e12418.
- Nopparat C, Sinjanakhom P, Govitrapong P. Melatonin reverses H<sub>2</sub>O<sub>2</sub>-induced senescence in SH-SY5Y cells by enhancing autophagy via siruin 1 deacetylation of the RelA/p65 subunit of NF-kappaB. 2017;63.
- Feng D, Wang B, Wang L et al. Pre-ischemia melatonin treatment alleviated acute neuronal injury after ischemic stroke by inhibiting endoplasmic reticulum stress-dependent autophagy via PERK and IRE1 signalings. *J Pineal Res* 2017;62:e12395.
- Areti A, Komirishetty P, Akuthota M et al. Melatonin prevents mitochondrial dysfunction and promotes neuroprotection by inducing autophagy during oxaliplatin-evoked peripheral neuropathy. *J Pineal Res* 2017;62:e12393.
- de Luxan-Delgado B, Potes Y, Rubio-Gonzalez A et al. Melatonin reduces endoplasmic reticulum stress and autophagy in liver of leptin-deficient mice. *J Pineal Res* 2016;61:108–123.
- Sauvageot CM, Stiles CD. Molecular mechanisms controlling cortical gliogenesis. *Curr Opin Neurobiol* 2002;12:244–249.
- Vazquez P, Arroba AI, Ceconi F et al. Atg5 and Ambra1 differentially modulate neurogenesis in neural stem cells. *Autophagy* 2012;8:187–199.
- Liang Q, Luo Z, Zeng J et al. Zika virus NS4A and NS4B proteins deregulate Akt-mTOR signaling in human fetal neural stem cells to inhibit neurogenesis and induce autophagy. *Cell Stem Cell* 2016;19:663–671.
- Agarwal S, Yadav A, Tiwari SK et al. Dynamin-related protein 1 inhibition mitigates bisphenol A-mediated alterations in mitochondrial dynamics and neural stem cell proliferation and differentiation. *J Biol Chem* 2016;291:15923–15939.
- Fonseca MB, Sola S, Xavier JM et al. Amyloid beta peptides promote autophagy-dependent differentiation of mouse neural stem cells: A beta-mediated neural differentiation. *J Biol Chem* 2013;48:829–840.
- Tabor-Godwin JM, Tsueng G, Sayen MR et al. The role of autophagy during coxsackievirus infection of neural progenitor and stem cells. *Autophagy* 2012;8:938–953.
- Moriya T, Horie N, Mitome M et al. Melatonin influences the proliferative and differentiative activity of neural stem cells. *J Pineal Res* 2007;42:411–418.
- Yang P, Shen WB, Reece EA et al. High glucose suppresses embryonic stem cell

differentiation into neural lineage cells. *Biochem Biophys Res Commun* 2016;472:306–312.

**37** Khacho M, Clark A, Svoboda DS et al. Mitochondrial dynamics impacts stem cell identity and fate decisions by regulating a nuclear transcriptional program. *Cell Stem Cell* 2016;19:232–247.

**38** Yang G, Cancino GI, Zahr SK et al. A Glo1-methylglyoxal pathway that is perturbed in maternal diabetes regulates embryonic and adult neural stem cell pools in murine offspring. *Cell Rep* 2016;17:1022–1036.

**39** Wang F, Xu C, Reece EA et al. Protein kinase C- $\alpha$  suppresses autophagy and

induces neural tube defects via miR-129-2 in diabetic pregnancy. 2017;8:15182.

**40** Piano I, Novelli E, Della Santina L et al. Involvement of autophagic pathway in the progression of retinal degeneration in a mouse model of diabetes. *Front Cell Neurosci* 2016;10:42.

**41** Ji L, Chen Z, Xu Y et al. Systematic characterization of autophagy in gestational diabetes mellitus. *Endocrinology* 2017;158:2522–2532.

**42** Dai X, Zeng J, Yan X et al. Sitagliptin-mediated preservation of endothelial progenitor cell function via augmenting autophagy

enhances ischaemic angiogenesis in. *Diabetes* 2018;22:89–100.

**43** Rezabakhsh A, Ahmadi M, Khaksar M et al. Rapamycin inhibits oxidative/nitrosative stress and enhances angiogenesis in high glucose-treated human umbilical vein endothelial cells: Role of autophagy. *Biomed Pharmacother* 2017;93:885–894.

**44** Romine J, Gao X, Xu XM et al. The proliferation of amplifying neural progenitor cells is impaired in the aging brain and restored by the mTOR pathway activation. *Neurobiol Aging* 2015;36:1716–1726.



See [www.StemCells.com](http://www.StemCells.com) for supporting information available online.